CONF-950798--1

LA-UR-95-2653

Title: STRUCTURE AND PROPERTIES OF METAL HYDRIDES PREPARED BY MECHANICAL ALLOYING

Author(s): Margot L. Wasz, CMS
Ricardo B. Schwarz, CMS

Submitted to: "Proccedings of the International Symposium on Metastable, Mechanically Alloyed, and Nanocrystalline Materials," Quebec, Canada, July 1995 (Trans Tech Publications)

MASTER

Los Alamos
NATIONAL LABORATORY

Form No. 836 R5
ST 2629 10/91

DISTRIBUTION OF THIS DOCUMENT IS UNLIMITED

STRUCTURE AND PROPERTIES OF METAL HYDRIDES PREPARED BY MECHANICAL ALLOYING

M. L. WASZ AND R. B. SCHWARZ
Center for Materials Science
Los Alamos National Laboratory
Los Alamos, NM 87545 U.S.A.

Keywords: mechanical alloying, metal hydrides, $LaNi_5$, hydrogen storage, intermetallics.

Abstract

Our research examines the structure and reversible hydrogen storage capacity of alloys based on the $LaNi_5$ intermetallic. The alloys are prepared by mechanical alloying (MA), a technique particularly useful when alloying $LaNi_5$ with low melting point elements such as tin and calcium. In $LaNi_{5-y}Sn_y$, x-ray diffraction and Rietveld analysis show that tin preferentially occupies the Ni(3g) sites in the $LaNi_5$ structure, and the unit cell volume increases linearly with tin content to a maximum tin solubility of 7.33 atomic percent ($LaNi_{4.56}Sn_{0.44}$). The addition of tin to $LaNi_5$ causes (a) a logarithmic decrease in the plateau pressures for hydrogen absorption and desorption, which is consistent with the corresponding increase in the volume of the $LaNi_5$ unit cell; (b) a decrease in the hysteresis between the pressures for hydride formation and decomposition, which is in agreement with a recent theoretical model for the effect; and (c) a linear decrease in the hydrogen storage capacity. Effect (c) is explained by a rigid-band model whereby electrons donated by the tin atoms occupy holes in the 3d band of $LaNi_5$, which could otherwise be occupied by electrons donated by the hydrogen atoms. Thermodynamic van't Hoff analysis for these alloys show an increase in hydride formation enthalpy and no change in entropy with increasing tin concentration. $LaNi_5$ with calcium additions shows enhanced kinetics of hydrogen absorption/desorption. The powder particles prepared by MA have a larger surface area than particles of the same overall size prepared by arc casting. All $LaNi_5$-based alloys prepared by MA in an inert environment require no activation for hydrogen absorption and suffer less comminution upon hydriding/dehydriding.

Introduction

Intermetallics based on $LaNi_5$ continue to generate interest for fuel cell and battery applications because they reversibly absorb large amounts of hydrogen at near ambient conditions of temperature and pressure. Furthermore, the hydriding characteristics of $LaNi_5$ can be easily altered through macroalloying, and the effects of various alloying elements are beginning to be understood. For example, rare earth elements substituted for the lanthanum modify the plateau pressure for hydride formation in proportion to the change in the $LaNi_5$ unit cell volume [1]. In addition, Ce substitution for La increases the kinetics for hydrogen absorption [2]. Substitutions for the nickel in the structure, like aluminum and indium, are known to lower the plateau pressures [3]. However, both substitutions also decrease the hydrogen storage capacity [4]. It has also been shown that aluminum limits the disproportionation of the alloy which occurs when these alloys are hydrided/dehydrided for many cycles [5 . Recently, $LaNi_{5-x}Sn_x$ was shown to suffer negligible losses in hydrogen storage capacity after 10,000 hydriding/dehydriding cycles in hydrogen gas [6]. This discovery motivated several studies to understand the basic mechanisms underlying the effect

of tin [7 ,8]. Finally, aluminum together with cobalt are usually added to $LaNi_5$ to increase its resistance to attack in electrochemical applications [9].

Because tin has a melting point of 232°C, and $LaNi_5$ melts congruently at 1325°C, it is not easy to fabricate this alloy by arc casting without running the risk of losing tin by evaporation and causing solute segregation during solidification. Similar restrictions apply to the synthesis of $LaNi_5$-based alloys containing calcium. The alloys studied in this work were prepared by MA, which permits easier alloy fabrication with less compositional uncertainties.

$LaNi_5$-based powders that have been stored in the presence of oxygen require surface activation in the form of high temperature vacuum annealing, or exposure to high hydrogen pressures, before they are able to absorb hydrogen to form hydrides. The effect of MA in an inert gas atmosphere with respect to surface activation is studied for these alloys.

One drawback in the use of $LaNi_5$ as a hydrogen storage material is the comminution of the alloy powder due to the 25% volume change of the material between hydride formation and decomposition [10]. Whether MA develops microstructures which better accommodate the volume change than arc cast material is also examined.

Experimental

$LaNi_{5-y}Sn_y$ (y = 0.0, 0.10, 0.29, and 0.39) alloy powders were produced by mechanical alloying #100 mesh, 99.5 % purity $LaNi_5$ powder (CERAC, Milwaukee, Wisconsin) with #100 mesh, 99.999% purity tin powder (AESAR, Ward Hill, Massachusetts). The powders were processed and handled in an argon glovebox containing less than 1 ppm oxygen. Alloys were mechanically alloyed for four hours using a SPEX 8000 mixer/mill, a tungsten carbide vial, and a single 12.1-gram tungsten carbide ball. The powders were then annealed in an open fused silica tube in the same glovebox at 800°C for 30 minutes. X-ray diffraction of the powders (XRD), described elsewhere [11], indicate that following the annealing all of the tin was incorporated either into the $LaNi_5$ structure or into a Ni(Sn) solid solution which precipitated to preserve the $La(Ni,Sn)_5$ stoichiometry. The compound, $La_{0.8}Ca_{0.2}Ni_{4.25}Co_{0.5}Sn_{0.25}$, was prepared by the same procedure, using 99.5% purity calcium shot (AESAR), and #100 mesh, 99.8 % purity cobalt powder (Alpha Chemicals, Danvers, Massachusetts).

The powders used to study hydrogen storage from the gas phase were sieved to particle sizes between 45μm to 150μm. One gram of alloy powder was mixed with an equal weight of copper powder to improve the thermal conductivity of the sample. This was necessary to minimize changes in temperature during hydride formation and dissolution. Alloys which were weighed, mechanically alloyed, and annealed in the glovebox, were also stored, sieved, and placed in the sample holder in the same glovebox without exposure to air.

The hydrogen storage characteristics were measured at 0°C using a computer-controlled Sieverts apparatus. For all compositions studied, the ball-milled alloys required no 'activation' by exposure to high hydrogen gas pressure or to high temperatures. We found, instead, that for the first three cycles, the absorption plateau pressures dropped slightly with the number of cycles and reached a constant value thereafter. Therefore, prior to measuring each pressure-composition isotherm, the alloys were charged and discharged five times between 5000 Torr and vacuum. At the conclusion of the pressure-composition measurements, absorption plateau pressures were measured at four different temperatures, ranging from 0°C and 40°C, for van't Hoff analysis. These pressures were measured at a constant hydrogen content near the midpoint of the absorption plateau, since previous research has shown that reaction enthalpies can vary across the plateau region [12].

The morphology of powder particles collected before and after hydrogen cycling were recorded with a JEOL JSM-6300FXV scanning electron microscope (SEM) equipped with a field emission gun.

Results

Analysis by XRD of the series $LaNi_5Sn_x$ (x=0 to 0.6) indicate that the $LaNi_5$ unit cell volume increases with increasing tin concentration to a maximum tin solubility of $LaNi_{4.56}Sn_{0.44}$, as shown in Figure 1. The lattice parameters *a* and *c* also increase linearly with increasing tin concentration to a maximum at the same tin concentration and are constant thereafter [13]. XRD of the alloys containing higher concentrations of tin also contain Bragg peaks corresponding of the compound $LaNi_5Sn$. $LaNi_5$ crystallizes in a hexagonal structure, group P6/mmm [14]. Nickel occupies two different sites, the 2c sites in the basal plane and the 3g sites in the intermediate plane (z = 1/2).

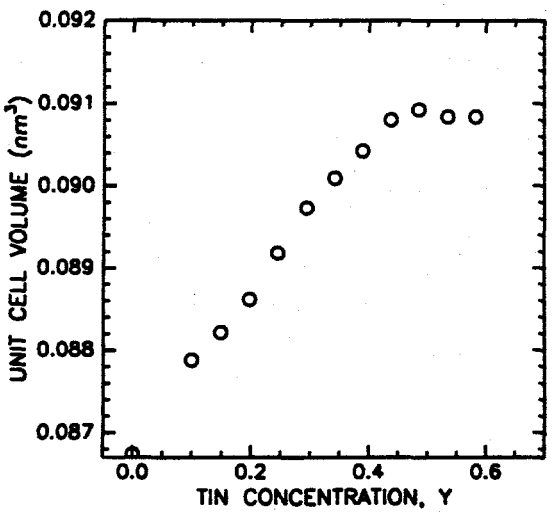

Figure 1 - $LaNi_{5-y}Sn_y$ unit cell volume as a function of tin content, y.

Rietveld analysis of the x-ray diffraction data for the $LaNi_{5-y}Sn_y$ series prepared by MA, described elsewhere [10], was refined with respect to the lattice position of the tin atoms, the lattice parameters, volume fraction of phases present, and particle-size distribution. Although the Rietveld analysis permitted the tin atoms to occupy any nickel or lanthanum lattice site in $LaNi_5$, in every case, the result of the optimization showed that the tin atoms occupy only the nickel 3g sites in the intermediate plane of the $LaNi_5$ unit cell.

Figure 2 shows the logarithm of the hydrogen absorption and desorption pressure plateaux as a function of tin content. The log of both plateau pressures decreases linearly with increasing tin content. Notice, however, that the difference in pressure plateaux, or pressure hysteresis, decreases with increasing tin content. The abscissa at the top of the figure shows the $LaNi_{5-y}Sn_y$ unit cell volume which is also proportional to the tin concentration, as shown in Figure 1. A similar dependence of the logarithm of the plateau pressure on unit cell volume was found by Mendelsohn and Gruen [1], who substituted different rare earth elements for lanthanum in $LaNi_5$.

The hydrogen storage capacity decreases with increasing tin content, Figure 3. These capacities were measured at pressures equal to six times the absorption pressure plateau of each alloy, listed in Table 1. This decrease in hydrogen storage capacity is not due to changes in interstitial site geometry because the $LaNi_5$ unit cell volume increases with tin content, Figure 1. We attribute the decrease in hydrogen storage capacity to changes in the $LaNi_5$ electronic band structure with Sn alloying, as discussed in the next section. It must be noted that the hydrogen storage capacity of $LaNi_5$ prepared by MA is less than that of arc cast $LaNi_5$, which is on the order of 6.7 mol H/mol $LaNi_5$ at 0°C. Using a mass spectrometer and a vacuum annealing furnace, we detected that the $LaNi_5$ powder prepared by MA evolved significant amounts of hydrogen and

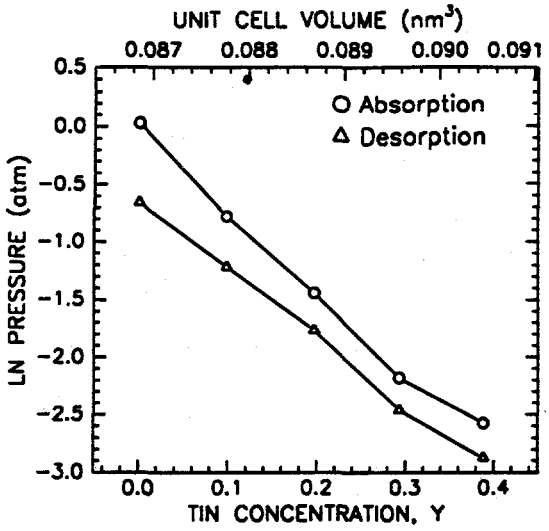

Figure 2 - Pressure plateaux as a function of tin content and unit cell volume.

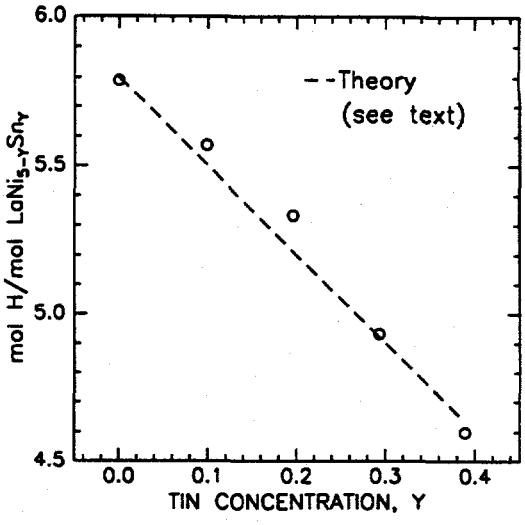

Figure 3 - Gas phase hydrogen capacity in $LaNi_{5-y}Sn_y$ as a function of tin content, y.

nitrogen when annealed at 200-400°C and 800-900°C, respectively. The gas trapped in the structure may have depressed the measured hydrogen storage capacity.

Table 1 summarizes the gas phase absorption/desorption characteristics of $LaNi_{5-y}Sn_y$ alloys prepared by MA, including the van't Hoff analysis. Note that the enthalpy for hydride formation decreases with increasing tin content but the entropy stays approximately constant. The measured entropy is largely that lost by the hydrogen gas as it enters the $LaNi_5$ lattice [15].

MA was also used to alloy $LaNi_5$ with another low melting point element, calcium. $La_{0.8}Ca_{0.2}Ni_{4.25}Co_{0.5}Sn_{0.25}$ was found to have extremely fast rates of hydrogen absorption. Figure 4 compares the pressure transients for hydrogen gas absorption in $La_{0.8}Ca_{0.2}Ni_{4.25}Co_{0.5}Sn_{0.25}$ and $LaNi_5Sn_{0.3}$. Initially, a reservoir in the Sieverts apparatus was charged to 9550 Torr of hydrogen.

Table 1 - Gas phase characterization of $LaNi_{5-y}Sn_y$

Alloy Composition	P_{abs} (Torr)	P_{des} (Torr)	Capacity at $6P_{abs}$ ($H/LaNi_{5-y}Sn_y$)	ΔH (kJ/mol H_2)	ΔS (J/mol H_2 K)
$LaNi_5$	785±14	396±3	5.789	28±6	104±20
$LaNi_{4.90}Sn_{0.10}$	350±8	226±4	5.570	31.3±3.8	107±13
$LaNi_{4.80}Sn_{0.20}$	180±2	130±2	5.333	32.4±2.0	106±7
$LaNi_{4.71}Sn0_{.29}$	86±5	65±2	4.931	32.8±0.6	102±2
$LaNi_{4.61}Sn_{0.39}$	58±8	43±3	4.598	34.6±0.2	104.0±0.6
$La_{0.8}Ca_{0.2}Ni_{4.25}Co_{0.5}Sn_{0.25}$	52±6	39±4	4.394	36.1±0.2	109.4±0.6

At time zero, a valve separating the gas reservoir and an evacuated reservoir containing the hydride-forming material was opened. Had no hydrogen been absorbed by the alloys, the pressure would have dropped to 7500 Torr. The difference between 7500 Torr and the final pressure of 5100 Torr measures the amount of hydrogen that was absorbed by the alloys. Note the high rate of hydrogen absorption in the $La_{0.8}Ca_{0.2}Ni_{4.25}Co_{0.5}Sn_{0.25}$ alloy, whereby 90% of the hydrogen is absorbed in less than five seconds.

The rate of hydrogen desorption in the calcium-containing alloys is also fast. Electrodes fabricated from these alloys, described elsewhere [12], were tested electrochemically. Figure 5 shows the discharge potential, measured at a constant discharge capacity of 100 mA h/g, as a function of discharge current. Note that the $La_{0.8}Ca_{0.2}Ni_{4.25}Co_{0.5}Sn_{0.25}$ alloy is able to maintain a much higher potential through the delivery of hydrogen than $LaNi_5Sn_{0.3}$.

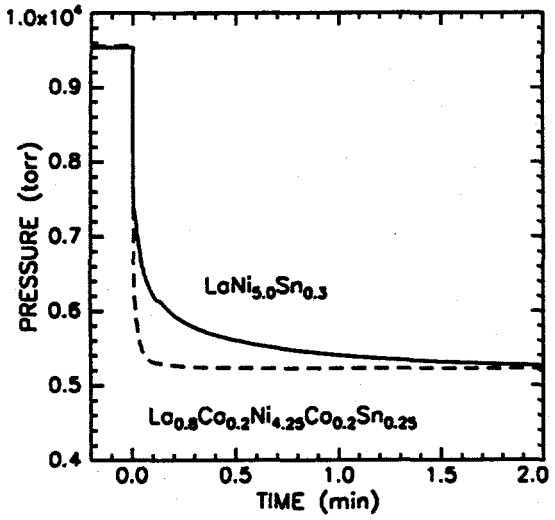

Figure 4 - Kinetics for hydrogen absorption of $La_{0.8}Ca_{0.2}Ni_{4.25}Co_{0.5}Sn_{0.25}$ and $LaNi_5Sn_{0.3}$.

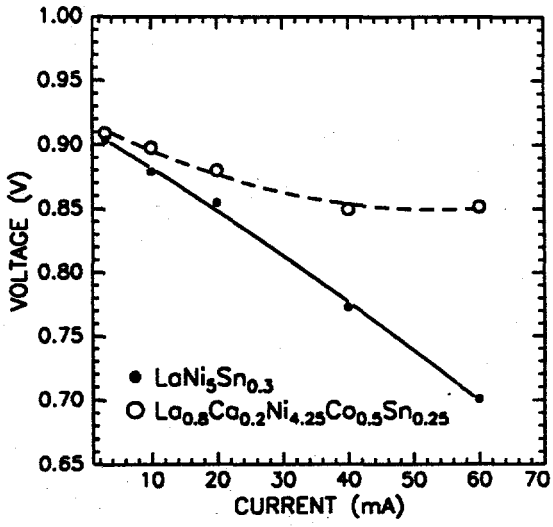

Figure 5 - Discharge potential, measured at a constant discharge capacity of 100 mA h/g, as a function of discharge current.

Various hydriding characteristics, such as kinetics of hydrogen absorption/desorption and rate of degradation during cyclic charging/discharging, are thought to depend on the powder particle morphology. Powder comminution upon hydrogen charging is thought to limit the lifetime of battery cells prepared from these materials. Figure 6 shows the typical shape of powder particles for cast $LaNi_5$, MA-$LaNi_5$, and MA-$LaNi_5Sn_{0.25}$. The left and right columns show the powder particles before and after charging with hydrogen, respectively. The cast powder particles have a sharp angular morphology, typical of fractured brittle materials, whereas the particles of powder prepared by MA have a rounded agglomerate morphology. After hydriding, the average size of the cast particles is significantly smaller. Those cast particles that do not fragment are heavily cracked. In contrast, the particles of powder prepared by MA seem to retain their size and morphology. Neither the $LaNi_5$ nor the $LaNi_5Sn_{0.25}$ powders prepared by MA show cracks following hydrogen charging. It thus appears that the powders prepared by MA can better accommodate the volume change caused by hydriding/dehydriding than do the cast alloys.

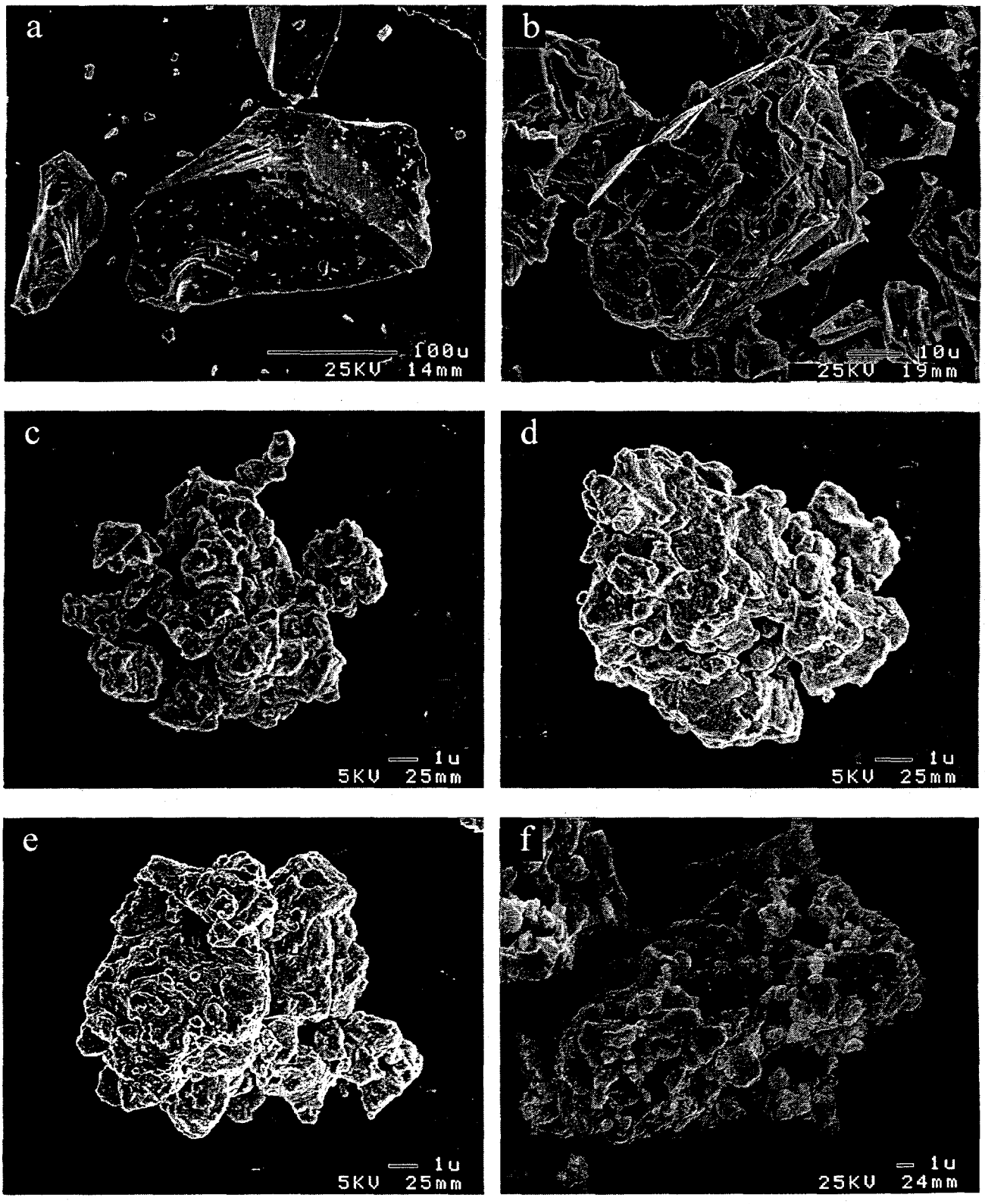

Figure 6 - SEM images of the powder microstructure of a) cast $LaNi_5$ before hydriding; b) cast $LaNi_5$ after 8 hydriding cycles; c) MA-$LaNi_5$ before hydriding; d) MA-$LaNi_5$ after 6 hydriding cycles; e) MA-$LaNi_5Sn_{0.25}$ before hydriding; and f) MA-$LaNi_5Sn_{0.25}$ after 8 hydriding cycles.

The SEM micrographs of Figure 6 cannot tell us conclusively whether the particles prepared by MA have internal cracks after hydrogen charging. To further compare the hydrogen-induced cracking in powder prepared by arc melting and MA, we measured the effective surface of the powders before and after hydrogen charging using BET analysis. In cast $LaNi_5$ alloy powder, the surface area was found to increase by $8x10^{-2}$ m^2/g between the first and second hydride cycle. In contrast, in mechanically alloyed $LaNi_5Sn_{0.25}$, the corresponding increase was only $1x10^{-3}$ m^2/g. These tests show that powders prepared by MA are less prone to fracture and comminution than arc cast powder upon hydrogen charging. However, it must be noted that the $LaNi_5$ undergoes a 25% volume change upon hydriding, whereas the volume change in the $LaNi_5Sn_{0.25}$ alloy is approximately 17% [16].

Discussion

The hydrogen storage capacity and pressure for hydride formation/decomposition in the mechanically alloyed powders agree with those measured earlier in powders prepared by arc casting [3].

The hydrogen storage capacity in tin-substituted $LaNi_5$ (Figure 3) decreases almost linearly with increasing tin concentration. This decrease can be explained by a simple filling of holes in the $LaNi_5$ 3d band by electrons donated by the tin solutes, as proposed by Gschneidner, et al. [17] for aluminum substituted $LaNi_5$. This filling decreases the number of holes that can be occupied by electrons from the hydrogen. The dashed line in Figure 3 is the hydrogen storage capacity calculated according to this model, assuming that each tin donates three electrons to the 3d band of $LaNi_5$. The agreement with the experimental data is good and well within experimental error.

The decrease in the pressure hysteresis with increasing tin concentration, Figure 2, agrees qualitatively with a recent theoretical model for the effect [18]. The model predicts,

$$\ln\frac{p_{abs}}{p_{des}} \propto \Delta c\left(\frac{\partial a}{a\partial c}\right)^2 \qquad (1)$$

where $(\partial\, a/a\partial\, c)^2$ is the logarithmic change in the lattice parameter, a, of the α-phase dilute metal-hydrogen solid solution with a change in the concentration of interstitial hydrogen atoms, c. There are no data for $\partial\, a/a\partial$ c in $LaNi_5$ and $LaNi_{5-y}Sn_y$ alloys. In a first approximation, we can assume that $\partial\, a/a\partial$ c equals Δa/[a Δc], where Δa is the difference between the lattice constants of the metal and hydride phases, and Δc is the hydrogen concentration in the hydride phase. Then, the right hand side of Equation (1) can be estimated from the reported change in the volume of the alloy upon hydride formation, 25% for $LaNi_5$ and 17% for $LaNi_{4.7}Sn_{0.3}$ [15]. The left hand side of Eq. 1 can be calculated from the data in Table 1. Evaluating Eq. (1) this way for $LaNi_5$ and for $LaNi_{4.7}Sn_{0.3}$, and taking the ratio, we obtain $ln(785/369)/ln(86/65) = 2.69$ for the left hand side, and $(0.25/0.17)^2(4.93/5.79) = 1.84$ for the right hand side. The agreement is not bad, considering the approximations taken.

Whereas commercial $LaNi_5$ alloy powder always requires a surface 'activation' before it can absorb large quantities of hydrogen reversibly, the $LaNi_5$-based alloys prepared by MA in an inert atmosphere require no surface activation. The difference in behavior could be due to two reasons: (1) the presence of nickel inclusions in the MA powders and (2) the presence of La oxides on the

surface of the commercial powder. All alloys prepared by MA contained trace amounts of a Ni(Sn) solid solution phase. Previous studies have shown that nickel segregation to the surface of $LaNi_5$ is important in the activation process [19]. Conversely, it is well known that La_2O_3 impedes hydrogen absorption. However, non-stoichiometric La-oxides are excellent catalysts for hydrogen dissociation, better in fact, than nickel oxide [20]. To test the influence of oxidation on the need of surface activation for hydrogen absorption, an arc cast single-phase $LaNi_5$ pellet was pulverized in the argon-atmosphere glovebox. This powder required no surface activation for hydride formation. Because this alloy had no Ni(Sn) second phase, it appears that the need of surface activation in the commercial $LaNi_5$ powders is due to the presence of surface oxides, formed, most likely, during storage and shipping.

Because the surface area is larger in the mechanically alloyed powders than in the arc cast powders, it is anticipated that hydriding/dehydriding will be faster in the powders prepared by MA. Figure 7 shows the hydrogen absorption kinetics of $LaNi_5$ powder prepared by arc casting and by MA. Note that there is a large change in the absorption kinetics between the first and fifth hydriding cycles in the cast $LaNi_5$ but relatively little change between the rate of hydrogen absorption in the $LaNi_5$ prepared by MA. This is probably because hydriding causes a drastic increase in the surface area density of the cast alloys, as seen in Figure 6 and demonstrated by the BET measurements.

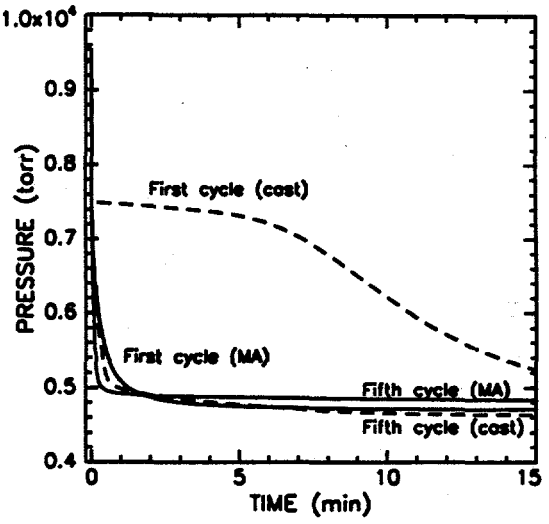

Figure 7 - Comparison of the kinetics of hydrogen absorption in as-cast and mechanically alloyed $LaNi_5$.

For practical applications of $LaNi_5$-based alloys (e.g., electrodes in Ni/metal hydride batteries), it is significant that alloys prepared by MA require neither surface activation nor hydrogen cycling to break down the powder to its terminal particle size. The morphology of the activation nor powder prepared by MA is nearly the same before and after hydrogen cycling, and hydride-induced cracking is minimal. The lack of hydride-induced cracking is partly due to the smaller initial particle size of the MA powders before hydriding, as well as the rounded agglomerate morphology that better accommodates the volume change caused by hydriding.

References

1 M. H. Mendelsohn and D. M. Gruen, Nature **269**, 45 (1977).

2 K. R. Clay, A. J. Goudy, R. G. Schweibenz, and A. Zarynow, J. Less-Comm. Met. **166**, 153 (1990).

3 M. Mendelsohn, D. Gruen, and A. Dwight, Inorganic Chemistry **18**, 3343 (1979).

4 D. G. Westlake, J. Less-Comm. Met. **91**, 1 (1983).

5 P. D. Goodell, J. Less-Comm. Met. **99**, 1 (1984).

6 S. W. Lambert, D. Chandra, and W. N. Cathey, J. of Alloys and Compounds **187**, 113 (1992).

7 J. S. Cantrell, T. A. Beiter, R. C. Bowman, Jr., J. Alloys and Comp., **207/208**, 372 (1994).

8 R. C. Bowman, Jr., C. H. Luo, C. C. Ahn, C. K. Witham, and B. Fultz., J. Alloys and Comp. **217**, 185 (1995).

9 J. J. G. Willems and K. H. J. Buschow, J. Less-Comm. Met. **129**, 13 (1987).

10 J. H. N. van Vucht, F. A. Kuijpers, and H. C. A. M. Bruning, Philips Res. Repts. **25**, 133 (1970).

11 M. L. Wasz, P. B. Desch, and R. B. Schwarz, submitted to Phil. Mag., 1995.

12 T. B. Flanagan, W. Luo, and J. D. Clewley, in Hydrogen Storage Material, Batteries, and Electrochemistry, edited by D. A. Corrigan and S. Srinivasan (The Electrochemical Society, Pennington, New Jersey, 1992), p. 46.

13 M. L. Wasz, R. B. Schwarz, S. Srinivasan, and M. P. S. Kumar, Mater. Res. Soc. Symp. Proc., Symposium on Materials for Electrochemical Energy Storage and Conversion - Batteries, Capacitors, and Fuel Cells, Spring 1995 Meeting, San Francisco.

14 K. H. Buschow and H. H. Van Mal, J. Less Comm. Met. **29**, 203 (1972).

15 H. H. Van Mal, K. H. J. Buschow, and A. R. Miedema, J. Less-Comm. Met. **35**, 65 (1974).

16 F. W. Oliver, W. Morgan, E. C. Hammond, S. Wood, and L. May, J. Appl. Phys. **57**, 3250 (1985).

17 K. A. Gschneidner, Jr., T. Takeshita, Y. Chung, and O. D. McMasters, J. Phys. F: Met. Phys. **12**, L1 (1982).

18 R. B. Schwarz and A. G. Khachaturyan, Phys. Rev. Lett. **74**, 2523 (1995).

19 L. Schlapbach, A. Seiler, F. Stucki, and H. C. Siegmann, J. Less-Comm. Met. **73**, 145 (1980).

20 H. Uchida, Y. Ohtani, M. Ozawa, T. Kawahata, and T. Suzuki, J. Less-Comm. Met. **172-174**, 983 (1991).